MLM-2302
TID-4500
UC-15

Nuclear Safeguards Progress Report: July-December 1975

Issued: April 2, 1976

R. P. Ratay, Editor

NOTICE

This report was prepared as an account of work sponsored by the United States Government. Neither the United States nor the United States Energy Research and Development Administration, nor any of their employees, nor any of their contractors, subcontractors, or their employees, makes any warranty, express or implied, or assumes any legal liability or responsibility for the accuracy, completeness or usefulness of any information, apparatus, product or process disclosed, or represents that its use would not infringe privately owned rights.

PRINTED IN THE UNITED STATES OF AMERICA

Available from
National Technical Information Service
U. S. Department of Commerce
5285 Port Royal Road
Springfield, Virginia 22161
Price: Printed Copy $4.00; Microfiche $2.25

MONSANTO RESEARCH CORPORATION
A Subsidiary of Monsanto Company

MOUND LABORATORY
Miamisburg, Ohio 45342
operated for

UNITED STATES ENERGY RESEARCH AND DEVELOPMENT ADMINISTRATION

U. S. Government Contract No. E-33-1-GEN-53

DISCLAIMER

Table of Contents

Development of Nondestructive Assay Techniques

PLUTONIUM ISOTOPIC MEASUREMENTS BY GAMMA-RAY SPECTROSCOPY

F. X. Haas and J. F. Lemming

INTRODUCTION

This section describes a continuing effort in the development of gamma-ray techniques for the measurement of plutonium and americium-241 isotopic concentrations. The overall goal of the project is to obtain these isotopic ratios to within a 3% error for the range of plutonium burnup and mixed oxide blends expected for power reactors. Previous work is described in a prior report.[1]

The primary efforts of the gamma-ray spectroscopic program in this reporting period have been focused on obtaining a complete set of isotopic data in the energy region from 120 to 450 keV. This portion of the spectrum has a high counting rate and would thus reduce the data acquisition time for analysis. The spectrometer systems and the equations necessary to convert peak areas to isotopic ratios are discussed in reference 1.

RESULTS

In order to demonstrate the use of the 120-450-keV region, the 1-cc Ge(Li) spectrometer was used to acquire ten spectra each for NBS-SRM-946, -947, and -948. Counting times of 20,000 sec per spectrum were used at count rates of 2,000 counts/sec in the spectrometer. Tables 1, 2, and 3 show the plutonium isotopic values obtained in the energy region from 148 to 208 keV of NBS-SRM-946, -947, and -948, respectively. The programs GRPANL[2] were used to extract the peak areas. Plutonium isotopics were calculated using the following peak ratios: the 153-keV/148-keV peaks for $^{238}Pu/^{241}Pu$; the 160-keV/164-keV peaks for $^{240}Pu/^{241}Pu$; and the 208-keV/203-keV peaks for $^{241}Pu/^{239}Pu$. The conversions to $^{238}Pu/^{239}Pu$ and $^{240}Pu/^{239}Pu$ are made using the $^{241}Pu/^{239}Pu$ measurements at 208 keV/203 keV. Consequently, any biases determined for the $^{241}Pu/^{239}Pu$ concentrations are transmitted to the other plutonium isotopic ratios. If the percent differences listed in the tables for $^{241}Pu/^{239}Pu$ are considered to be biases, and if they are removed, then the isotopic values agree with the NBS listed values to within ±5%. The one exception is the plutonium-238 value for NBS-SRM-948 which would be 9% high. This discrepancy with the listed value is consistent with our past results[1,3] and with gamma-ray spectroscopic values determined at LASL.[4]

The results shown in the tables for the NBS-SRM standards are comparable to these obtained using the 70-cc Ge(Li) spectrometer for plutonium-238 and plutonium-241 concentrations. Attempts to use the 160-keV region with spectra obtained on the 70-cc Ge(Li) spectrometer yielded results which were 20% to 30% below accepted values for NBS-SRM, Metal Exchange, and Inventory Verification samples.[1] These biases do not exist when using spectra acquired with the smaller detector with its better resolution.

Isotopic ratios of americium-241 have been calculated using three energy regions in spectra accumulated on the 1-cc planar Ge(Li) detector: (a) the 125-keV/129-keV peak ratio; (b) the 169-keV/171-keV peak ratio; (c) the energy region from 332 to 335 keV.[1] The average $^{241}Am/^{239}Pu$ isotopic ratios obtained from these regions are shown in Table 4 together with the value obtained from the 662-keV/659-keV peak ratio using the 70-cc Ge(Li) spectroscopy system. This value is used as a basis of comparison since the NBS samples are not certified for americium content. The values obtained from the 125-keV/129-keV and 169-keV/171-keV peaks agree with the 662-keV/659-keV value to within 2% for all samples with a standard deviation of the average of 2% or less for the 125-keV/129-keV ratio and 8 to 12% for the 169-keV/171-keV ratio. As

Table 1

COMPARISON OF GAMMA-RAY AND CERTIFIED VALUES FOR NBS-SRM-946
(NOVEMBER 1975)

Plutonium Isotopic Ratio	NBS Value (ppm)	Gamma Value (ppm)	Difference (%)	Standard Deviation (%)
238/239	2877 ± 82	2799 ± 62	-2.7	2.2
240/239	145140 ± 180	151345 ± 18715	4.3	12.4
241/239	39610 ± 50	40452 ± 1345	2.1	3.3

Table 2

COMPARISON OF GAMMA-RAY AND CERTIFIED VALUES FOR NBS-SRM-947
(NOVEMBER 1975)

Plutonium Isotopic Ratio	NBS Value (ppm)	Gamma Value (ppm)	Difference (%)	Standard Deviation (%)
238/239	3787 ± 77	3907 ± 112	3.2	2.9
240/239	241522 ± 290	263177 ± 31844	9.0	12.1
241/239	49478 ± 65	52115 ± 2380	5.3	4.6

Table 3

COMPARISON OF GAMMA-RAY AND CERTIFIED VALUES FOR NBS-SRM-948
(NOVEMBER 1975)

Plutonium Isotopic Ratio	NBS Value (ppm)	Gamma Value (ppm)	Difference (%)	Standard Deviation (%)
238/239	117 ± 11	126 ± 13	7.6	10.2
240/239	86401 ± 110	83236 ± 12070	-3.7	14.5
241/239	4420 ± 10	4360 ± 53	-1.4	1.2

Table 4

$^{241}Am/^{239}Pu$ ISOTOPICS FROM DIFFERENT PEAK AREA DETERMINATIONS

Sample	662-keV/659-keV Value [70-cc Ge(Li)]	125-keV/129-keV Value [1-cc Ge(Li)]	169-keV/171-keV Value [1-cc Ge(Li)]	330-keV Region [1-cc Ge(Li)]
NBS-SRM-946	12100 ± 570[a]	11905 ± 140	12005 ± 1010	12245 ± 5290
NBS-SRM-947	13030 ± 590	13270 ± 175	13095 ± 1055	17390 ± 2780
NBS-SRM-948	3525 ± 55	3460 ± 75	3535 ± 450	4030 ± 1005

[a] Values are in parts per million.

has been pointed out earlier,[1] the 169-keV/171-keV ratio can be used only for americium-241 concentrations greater than 1000 ppm relative to plutonium-239.

The americium-241 concentrations could not be obtained at 125 keV with the 70-cc Ge(Li) spectrometer because of insufficient resolution in this region. The results at high concentration of americium using the 1-cc Ge(Li) spectrometer agree very well with the results obtained at 662 keV as shown in Table 4. However, this low-energy region still needs to be tested at low concentrations of americium-241.

The 1-cc planar detector has been used to analyze the 330-keV region to obtain $^{241}Pu/^{239}Pu$ and $^{241}Am/^{239}Pu$ ratios. The ^{241}Pu values calculated are on the order of 30% below the listed values for the NBS-SRM samples, with standard deviations of the averages ranging from 16% to 43%. Gunnink's simulation studies[6] predict a reproducibility of 10% or better for this region with an americium-241 concentration equal to the ingrowth obtained from pure plutonium material at the end of 1 yr. Our NBS-SRM samples do not fit this criterion.

In order to build confidence in the 120 to 400-keV energy region and to investigate the 330-keV region with samples having low americium-241 content, the isotopic ratios for the next Inventory Verification Sample Exchange will be measured on both the 1-cc Ge(Li) and the 70-cc Ge(Li) spectrometers. This will give sufficient data on larger samples to make a statistical evaluation of the system for the measurement of bulk samples around which the Mound Laboratory Safeguards program is centered.

In addition to the analysis of spectra acquired on the 1-cc detector, the 640-keV/639-keV peak ratios for data acquired with the 70-cc Ge(Li) spectrometer have been analyzed for $^{240}Pu/^{239}Pu$ concentrations. Both of these gamma rays have weak branching intensities, and there are several americium-241 peaks which contribute to the background in this area. In spite of these difficulties, this peak pair has given favorable results on a number of samples which have high count rates. The analysis of five ZPPR fuel pins (86% ^{239}Pu; 11.5% ^{240}Pu) yields a $^{240}Pu/^{239}Pu$ ratio which differs from chemical analysis by less than 1%. The standard deviation about the mean for these five pins is 6%.

The analysis of 23 analytical aliquots from the Inventory Verification Program on weapons-grade material containing approximately 93% plutonium-239 yields $^{240}Pu/^{239}Pu$ ratios 7% lower than the mass spectrometer values. These measurements have a precision of 11%.

In an attempt to improve the $^{240}Pu/^{239}Pu$ ratio determination using the 600-keV region, data were accumulated for up to 72 hr on 0.25-g NBS-SRM-946, -947, and -948. Because the peak-to-background ratio is small for these samples, the uncertainties on peaks supplied by the stripping program were on the order of 10%. For these particular samples this appears to be the practical limit.

Present attempts to extract the $^{240}Pu/^{239}Pu$ ratio at 640 keV from a bulk 254-g sample of PuO_2 containing 23% plutonium-240 are yielding preliminary results which are 17% below the chemical analysis values supplied with the sample.

PREDICTION OF CALORIMETER EQUILIBRIUM

C. L. Fellers and
P. W. Seabaugh

INTRODUCTION

A series of tests is being conducted in an attempt to verify a mathematical technique for predicting the equilibrium value of a calorimeter. This type of theoretical study can be not only useful in reducing sample turnaround time but may provide information that can be used to improve future calorimeter designs.

TEST DESCRIPTION

The verification tests are being conducted in a standard Mound Laboratory Model 100 calorimeter (S/N 106) with a sample chamber 1 in. x 3 in. (2.5 cm x 7.5 cm). This resistance-bridge calorimeter has a sensitivity of approximately 120,000 μV/W with a constant bridge current of 5 mA. The bridge potential is measured at 30-sec intervals by a Hewlett-Packard 3490A digital voltmeter and the data are recorded on magnetic tape interfaced with an HP-9820 calculator.

Duplicate runs have been conducted for each of six different tests. The tests consist of thermally disturbing the calorimeter and continually monitoring the bridge potential until an equilibrium condition is obtained. They are described below.

1. Empty sample container
   Starting condition: bath temperature (baseline)
   Thermal disturbance: 1-W internal heater turned "on"
   Final condition: 1-W equilibrium

2. Empty sample container
   Starting condition: 1-W equilibrium
   Thermal disturbance: heater turned "off"
   Final condition: baseline

3. Sample container filled with lead shot
   Starting condition: baseline
   Thermal disturbance: 1-W heater "on"
   Final condition: 1-W equilibrium

4. Sample container filled with lead shot
   Starting condition: 1-W equilibrium
   Thermal disturbance: heater turned "off"
   Final condition: baseline

5. One-watt plutonium-238 standard in sample container filled with lead shot
   Thermal disturbance: container and sample placed in calorimeter after being heated with hot air
   Final condition: 1-W equilibrium

6. One-watt plutonium-238 standard in sample container filled with lead shot
   Thermal disturbance: container and sample at room temperature placed in calorimeter
   Final condition: 1-W equilibrium

MATHEMATICAL TECHNIQUE

When a source of constant power is placed in a calorimeter, the bridge potential tends toward an equilibrium condition on an exponential curve. The initial portion of the equilibrium curve is composed of several exponential terms as shown in Equation 1.

$$y = A + Be^{-\lambda_1 t} + Ce^{-\lambda_2 t} + De^{-\lambda_3 t} + \ldots \quad (1)$$

However, the curve rapidly conforms to a single exponential equation.

The mathematical form used to predict equilibrium values for the initial series of tests is applicable only to the case where a single exponential sufficiently describes the equilibrium curve (Equation 2):

$$y = A + Be^{-\lambda t} \quad (2)$$

Other forms, including multiple exponential, are also under consideration. In Equation 2 the exponential term $Be^{-\lambda t}$ goes to zero, and y, the observed data, equals the equilibrium value A as t (time) approaches infinity. Since there are three unknowns in Equation 2, any three equally spaced points on the equilibrium curve can be used to predict A as shown in the following example:

Three equally spaced data points are represented by Equations 3, 4, and 5 where ϵ is the time interval between points.

$$y_1 = A + B\exp(-\lambda t) \quad (3)$$

$$y_2 = A + B\exp(-\lambda t + \lambda\varepsilon) \quad (4)$$

$$y_3 = A + B\exp(-\lambda t + 2\lambda\varepsilon) \quad (5)$$

Taking the natural logarithms of each equation yields the following set of equations:

$$\ln(y_1 - A) = \ln(B) - \lambda t \quad (6)$$

$$\ln(y_2 - A) = \ln(B) - \lambda t + \lambda\varepsilon \quad (7)$$

$$\ln(y_3 - A) = \ln(B) - \lambda t + 2\lambda\varepsilon \quad (8)$$

Solve Equations 6, 7, and 8 for $(y_3 - A)$:

$$\ln(y_3 - A) = 2\ln(y_2 - A) - \ln(y_1 - A) \quad (9)$$

$$y_3 - A = \frac{(y_2 - A)^2}{(y_1 - A)} \quad (10)$$

Expand Equation 10:

$$y_1 y_3 - y_1 A - y_3 A + A^2 = y_2^2 - 2y_2 A + A^2 \quad (11)$$

Solve for A:

$$A = \frac{y_2^2 - y_1 y_3}{2y_2 - y_1 - y_3} \quad (12)$$

A nonlinear convolution was used to smooth the data from the 12 test runs before equilibrium values were predicted using Equation 12.

DATA ANALYSIS

Data were collected on a 30-sec interval, but were analyzed on 30, 60, and 90-sec intervals. Consider the following sequence of data collection:

$$y_1, y_2, y_3, y_4, y_5, \ldots y_n$$

Each successive point is spaced 30-sec apart. Values are predicted using succesive three-point intervals by the following equations:

Thirty-second interval:

$$A_i = \frac{y_{i+1}^2 - y_i y_{i+2}}{2y_{i+1} - y_i - y_{i+2}} \quad (13)$$

$$i = 1,\ldots,n-2$$

Sixty-second interval:

$$A_j = \frac{y_{j+2}^2 - y_j y_{j+4}}{2y_{j+2} - y_j - y_{j+4}} \quad (14)$$

$$j = 1,\ldots,n-4$$

Ninety-second interval:

$$A_k = \frac{y_{k+3}^2 - y_k y_{k+6}}{2y_{k+3} - y_k - y_{k+6}} \quad (15)$$

$$k = 1,\ldots,n-6$$

Figures 1 through 6 are plots of the raw data equilibrium curves and the predicted values for test 5, run A and test 6, run B.

Plots of the data analyzed at 30, 60, and 90-sec intervals are shown. If the raw data are following a single exponential, the predicted values should lie on a straight line parallel to the x-axis. It is obvious from the graphs that the predicted values are not consistently repeating for 10 to 15 min after loading of the sample. After this time, all internal portions of the calorimeter and sample are at equilibrium with each other. The calorimeter, however, is still approaching equilibrium with the water bath following a single exponential curve.

Tables 5, 6, and 7 list the results of the twelve runs. Each set of data was analyzed at three time intervals and the analyses were started only after the bridge potential was following a single exponential.

Table 8 presents data from test 6, run B analyzed on a 60-sec interval. These data are typical of all test results. The weighted average of the predicted value at the corresponding time from t_o is shown along with the percent deviation from the true equilibrium value. The predicted values are weighted in the following manner:

$$\text{Weighted average} = \sum_{i=1}^{n} (P_i)i \Big/ \sum_{i=1}^{n} i \quad (16)$$

where P is the individual predicted value. Also shown in Table 8 are the raw data at the corresponding time from t_o and their percent deviation from the true equilibrium.

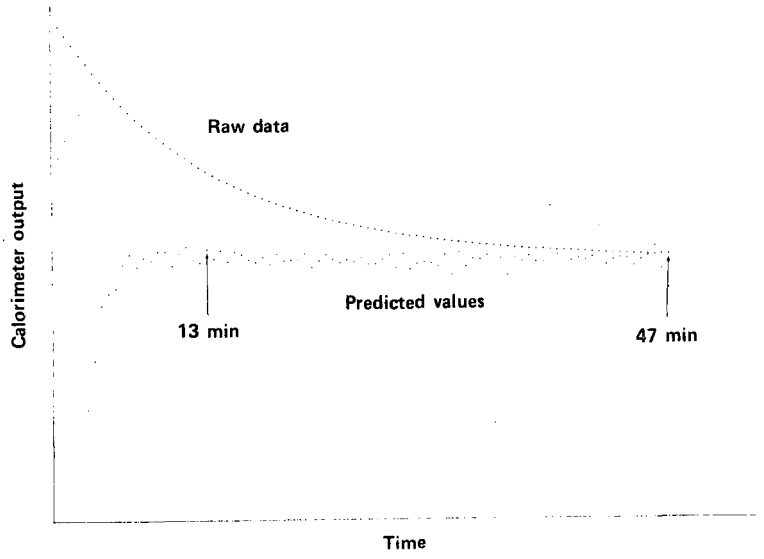

FIGURE 1 - Predicted and actual calorimeter outputs for test 5A analyzed on a 30-sec interval.

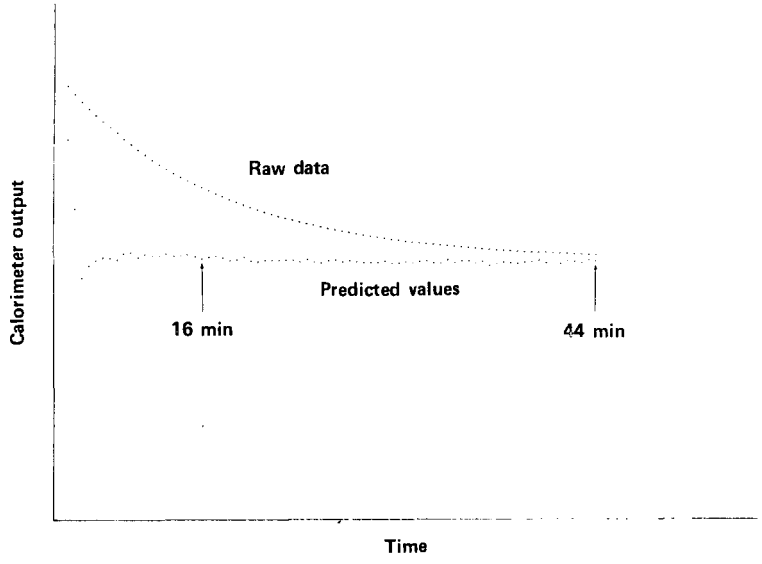

FIGURE 2 - Predicted and actual calorimeter outputs for test 5A analyzed on a 60-sec interval.

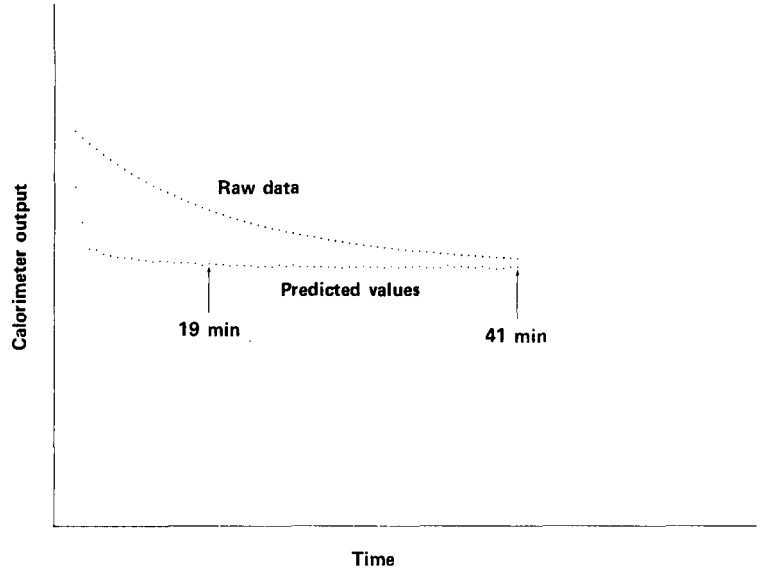

FIGURE 3 - Predicted and actual calorimeter outputs for test 5A analyzed on a 90-sec interval.

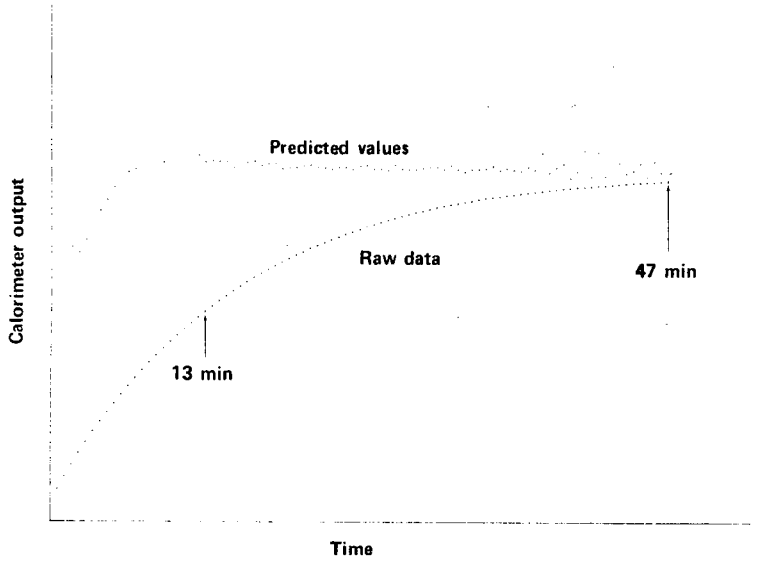

FIGURE 4 - Predicted and actual calorimeter outputs for test 6B analyzed on a 30-sec interval.

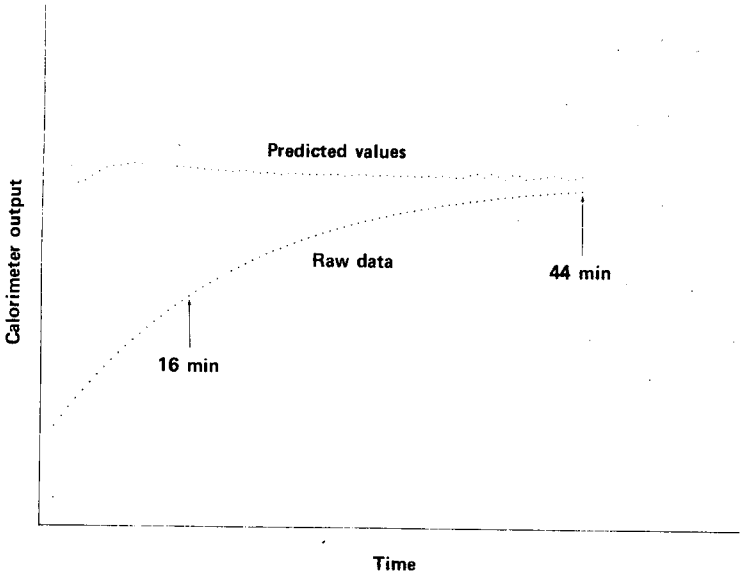

FIGURE 5 - Predicted and actual calorimeter outputs for test 6B analyzed on a 60-sec interval.

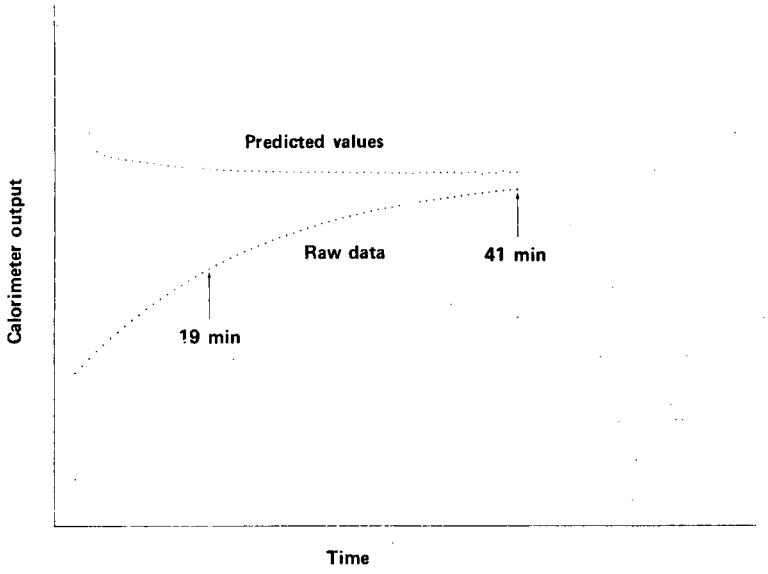

FIGURE 6 - Predicted and actual calorimeter outputs for test 6B analyzed on a 90-sec interval.

Table 5

PREDICTED CALORIMETER OUTPUT VERSUS TIME FOR TESTS 1A, 1B, 2A AND 2B

Time Interval (sec)	Time Span (min)	Average Predicted Value (μV)	Standard Deviation (μV)	Standard Deviation of Mean (μV)	Actual Equilibrium (μV)	Time to Equilibrium (Within 0.1%) (min)
Test 1, Run A						
30	13 - 42.5	120285	±2328	±303	120540	55
60	16 - 39.5	120567	±54	±7.9	120540	55
90	19 - 36.5	120554	±28	±4.9	120540	55
Test 1, Run B						
30	13 - 41.5	120593	±159	±21	120570	56
60	16 - 38.5	120569	±56	±8.4	120570	56
90	19 - 35.5	120558	±31	±5.5	120570	56
Test 2, Run A						
30	13 - 47	36	±163	±19	87	87
60	16 - 44	64	±50	±6.7	87	87
90	19 - 41	73	±30	±4.5	87	87
Test 2, Run B						
30	13 - 43.5	57	±133	±17	96	95
60	16 - 40.5	73	±50	±7.2	96	95
90	19 - 37.5	81	±24	±3.9	96	95

Table 6

PREDICTED CALORIMETER OUTPUT VERSUS TIME FOR TESTS 3A, 3B, 4A AND 4B

Time Interval (sec)	Time Span (min)	Average Predicted Value (μV)	Standard Deviation (μV)	Standard Deviation of Mean (μV)	Actual Equilibrium (μV)	Time to Equilibrium (Within 0.1%) (min)
Test 3, Run A						
30	13 - 47	120637	±335	±40	120560	90
60	16 - 44	120589	±118	±16	120560	90
90	19 - 41	120572	±75	±11	120560	90
Test 3, Run B						
30	13 - 47	119639	±867	±105	120560	90
60	16 - 44	120589	±149	±20	120560	90
90	19 - 41	120571	±77	±11	120560	90
Test 4, Run A						
30	13 - 47	24	±297	±36	81	115
60	16 - 44	46	±115	±15	81	115
90	19 - 41	64	±52	±7.9	81	115
Test 4, Run B						
30	13 - 47	16	±322	±39	85	110
60	16 - 44	55	±97	±13	85	110
90	19 - 41	71	±45	±6.9	85	110

Table 7

PREDICTED CALORIMETER OUTPUT VERSUS TIME FOR TESTS 5A, 5B, 6A AND 6B

Time Interval (sec)	Time Span (min)	Average Predicted Value (μV)	Standard Deviation (μV)	Standard Deviation of Mean (μV)	Actual Equilibrium (μV)	Time to Equilibrium (Within 0.1%) (min)
Test 5, Run A						
30	13 - 47	124343	±469	±57	124440	80
60	16 - 44	124658	±423	±57	124440	80
90	19 - 41	124622	±243	±37	124440	80
Test 5, Run B						
30	13 - 47	124409	±1472	±179	124440	100
60	16 - 44	124609	±310	±41	124440	100
90	19 - 41	124602	±198	±30	124440	100
Test 6, Run A						
30	13 - 47	124196	±1960	±238	124420	90
60	16 - 44	124405	±194	±26	124420	90
90	19 - 41	124422	±89	±13	124420	90
Test 6, Run B						
30	13 - 47	124947	±3338	±405	124400	95
60	16 - 44	124616	±380	±51	124400	95
90	19 - 41	124567	±203	±31	124400	95

Table 8

PREDICTED AND ACTUAL CALORIMETER OUTPUT VERSUS TIME FOR TEST 6B

Time from t_o[a] (min)	Number of Points	Weighted Average[b] (μV)	Standard Deviation (μV)	Standard Deviation of Mean (μV)	Deviation of Predicted Values from Equilibrium (%)	Raw Data	Deviation of Raw Data from Equilibrium (%)
20	4	125410	±166	±83	0.81	107097	-13.9
21	6	125237	±254	±103	0.67	108414	-12.9
22	8	125227	±226	±78	0.67	109638	-11.9
23	10	125086	±290	±92	0.55	110761	-11.0
24	12	124997	±312	±90	0.48	111807	-10.1
25	14	124899	±350	±94	0.40	112770	-9.3
26	16	124858	±347	±87	0.37	113661	-8.6
27	18	124808	±352	±83	0.33	114484	-8.0
28	20	124768	±354	±79	0.30	115247	-7.4
29	22	124719	±365	±78	0.26	115945	-6.8
30	24	124694	±362	±74	0.24	116597	-6.3
31	26	124667	±362	±71	0.21	117198	-5.8
32	28	124648	±358	±68	0.20	117751	-5.3
33	30	124618	±361	±66	0.18	118260	-4.9
34	32	124597	±360	±64	0.16	118732	-4.6
35	34	124579	±358	±61	0.14	119170	-4.2
36	36	124562	±357	±59	0.13	119570	-3.9
37	38	124529	±365	±59	0.10	119941	-3.6
38	40	124523	±362	±57	0.10	120290	-3.3
39	42	124532	±361	±56	0.11	120600	-3.1
40	44	124553	±355	±54	0.12	120900	-2.8
41	46	124532	±371	±55	0.11	121170	-2.6
42	48	124516	±379	±55	0.09	121400	-2.4
43	50	124491	±383	±54	0.07	121640	-2.2
44	52	124499	±376	±52	0.08	121860	-2.0
45	54	124477	±381	±52	0.06	122040	-1.9
46	56	124468	±380	±51	0.06	122230	-1.7

[a] Time to 0.1% of Equilibrium: 95 min.

[b] Actual Equilibrium: 124400 μV.

FUTURE WORK

This technique has proved to be successful in significantly reducing the time required to calorimetrically analyze a sample. However, all of these tests have been conducted in a relatively small calorimeter. Similar tests must be conducted on calorimeters of varying dimensions using different sample packaging configurations to determine the general usefulness of the approach. In addition, a sensitivity analysis will be conducted to determine the optimum sampling rate. Sensitivity analysis also will be used to check the consistency of multiple exponentials and data precision. Other techniques will be employed to determine when the data begin to follow a single exponential form.

AUTOMATED PLUTONIUM ASSAY SYSTEM

R. A. Neff, J. F. Lemming, J. H. Birden, T. K. Ferguson, D. O. Page, C. L. Fellers, and M. F. Duff

INTRODUCTION

The Automated Plutonium Assay System (APAS) is being developed to demonstrate automated, in-line, nondestructive plutonium assay for mixed oxide fuels. A process control computer will direct and control the movement of the samples from the storage area to the measurement stations. The data acquired by the computer will be immediately processed and will help provide material control and safeguards accountability.

AUTOMATION

Transport System

The three-dimensional (X,Y,Z) transporter has been installed in a test frame which simulates the APAS glovebox line. Figure 7 is a photograph of the test frame. The open design of the test stand allows evaluation and modification of components which cannot be easily viewed or accessed in the gloveboxes.

The transporter is being tested under computer control. For the purposes of these tests, a software package has been written for execution on a PDP-8/E computer. This program will allow thorough testing of the transporter and its controlling equipment prior to installation in the glovebox line.

The software program features an initialization routine which directs the return of all three axes to exact reference points. Another feature of the test program is that it allows the setting of as many as 20 positions in a cycle to be executed sequentially by the transport mechanism. The cycle can be halted after one execution or it can be repeated indefinitely. This feature is being used to determine life cycles of components and to check for any accumulative positioning errors.

Tests have been completed to determine the accuracy in the positioning of the transporter. A closed-loop control system is used to compensate for any drive backlash or wear in the system and to guarantee the accuracy and repeatability of each move. Figure 8 is a flow diagram of the control software. Optical shaft encoders on each of the three driven members are used to monitor the actual movement of the transport mechanism by simultaneously sending a proportional number of encoder pulses to the controller. The computer is used to compare this number with the move command it had originally transmitted and, if any difference exists, a correctional move command is transmitted.

Preliminary testing has shown that this automatic position correcting control brings the transporter within one stepping motor pulse (the smallest possible increment of motor revolution) of the exact coordinates in every axis. The inherent backlash of a direction change is effectively nullified. During these tests simulated plutonium containers were routinely placed in tubes (representing assay device or storage chamber openings) having only 0.10-mm diametral clearances.

In order to prevent inertial jerking of the load, the stepping motors have been programmed with speed control ramps for the first and last 1000 pulses of a move. Figure 9 is a plot of the control ramp. These ramps allow a gentle pickup and release of the containers during the operation of the Z-axis (vertical) drive. They also help to prevent swaying in the X and Y axes.

Additional tests are being conducted to evaluate the pickup devices (page 20) in order to develop statistical data on repeatability and to establish life cycle figures for the wear components of the system.

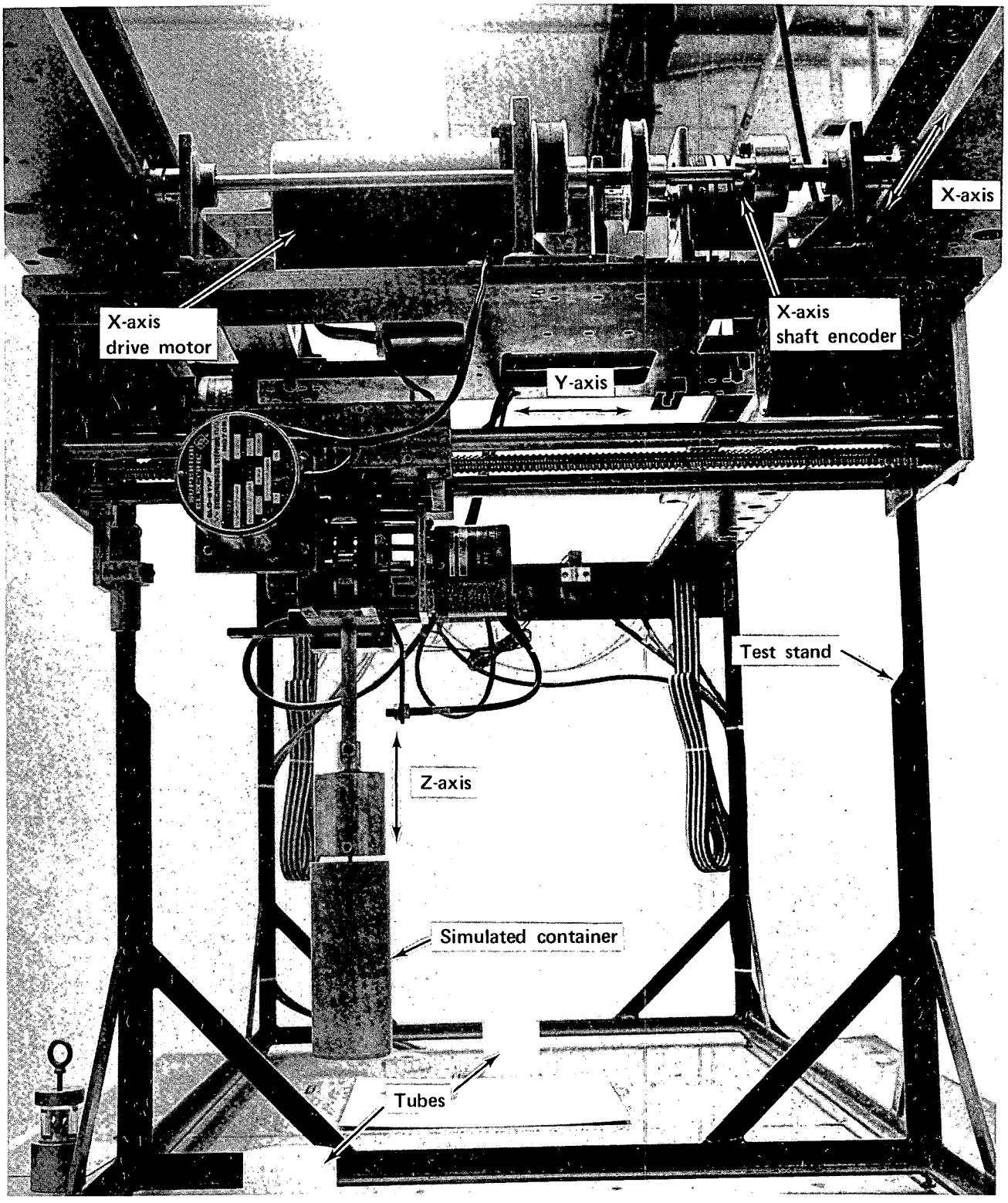

FIGURE 7 - Transporter mounted on a test stand for easy accessibility.

751116

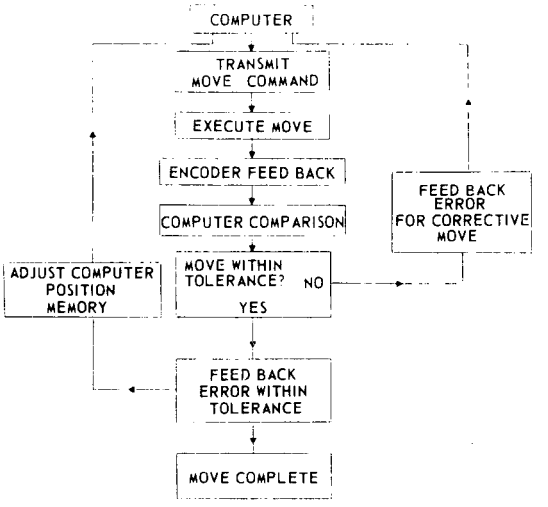

FIGURE 8 - Flow diagram of control software.

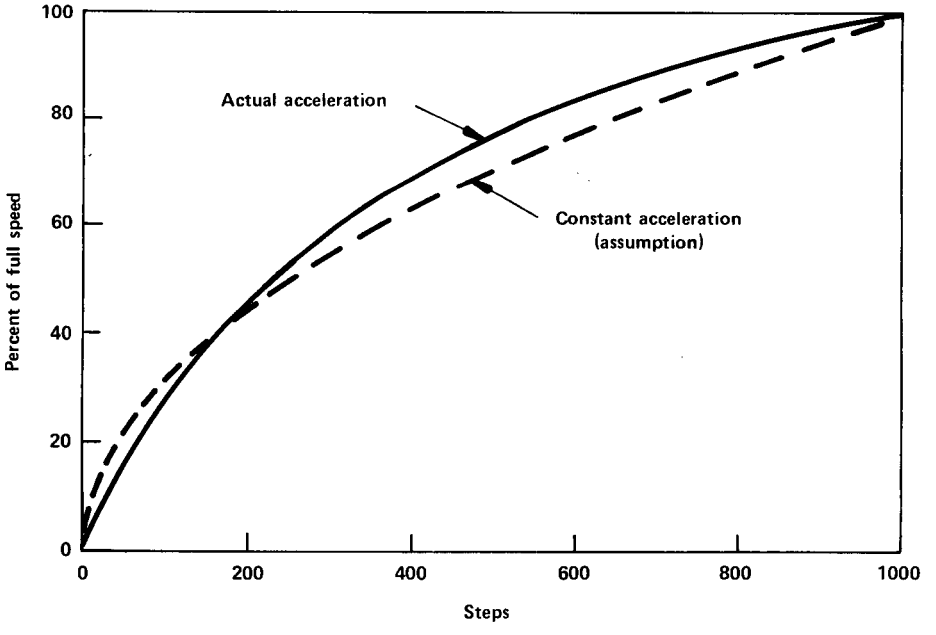

FIGURE 9 - Stepping motor drive curve.

Computer

The multichannel analyzer for the gamma-ray spectrometer has been interfaced to the PDP-11 computer. The handlers and drivers for this system and the X,Y,Z transporter are now being written.

Container Identification System

Two companies were solicited for their theoretical approach to solving the container identification problem. The specified guidelines required reading the information on a 1-3/4-in. (44.45-mm) diameter flat surface through a 3/8-in. (9.52-mm) safety plate glass and from a distance of 4 ft (1.2 m). Further, the scanner must be able to read the container in any radial alignment and have an extremely high reliability factor which will be determined exactly at a later date. The reading time, which is not critical, was specified as "a few seconds." The hardware supplied by the two companies is quite similar and it is only in the approach to the solution of the problem that they differ.

Company A suggests an "L"-shaped label with redundant information on each leg. This arrangement would permit the information to be read by one laser scanner because of the scanner's angle of readability. (The scanner can read information which is misaligned ±45°.) This approach to the problem would probably limit the number of digits to three. Company B would use an "in-line" label with a dual-beam scanner. In this arrangement, the two beams scan the information at right angles to each other. Again, the angle of readability permits the container to be identified in any radial alignment. This approach to the problem, although somewhat more expensive, would accommodate four or perhaps five digits.

Pickup Device Evaluation

A testing system (see Figure 10) for determining the reliability of potential pickup devices was assembled and used to evaluate two pickup devices. The system was designed to cycle the pickup devices at a moderate rate (15-20 cycles/min) and to register the latching failures, unlatching failures, and accumulated cycles. The first device tested was a small, commercially available dual-state mechanism. It was cycled on the testing system approximately 20,000 times and the results showed two possible failure modes. Failures tended to occur in batches (8 or 10 failures in 25 cycles) and then testing would go for several hundred cycles with no failures. However, when this pickup device was installed on the transport mechanism, the failures tended to occur at more regular intervals of perhaps 1 in 50 cycles.

The second device tested was designed to handle the reusable stainless steel calorimeter can described on page 22. This device was run on the testing rig for approximately 2500 cycles and then modified to correct deficiencies which showed up. It was then cycled approximately 10,000 additional times with a failure rate of zero. It was installed on the transport mechanism and has yet to fail in about 3 days of random testing. Although the second pickup device has a tendency to twist upon actuation, this does not seem to affect its working efficiency.

CALORIMETRY

Process Calorimeters

Tests have been conducted on the two APAS calorimeters (serial numbers 160 and 161) to determine the characteristics of the thermal gradient media. The sensitivity of the calorimeter, the time to reach equilibrium, and the output stability are directly related to the physical parameters of the thermal resistance across which heat must flow (Figure 11). As mentioned in a previous report,[1] various materials (silicone greases, oils, and sand) were tested for their mechanical properties when filling the gap. Banding sand was selected originally as the gradient medium because it has a thermal conductivity nine times that of air and could be easily removed from the gap if necessary. Significant heat distribution errors and output instability were encountered with sand in the gradient gap. It was discovered that the sand could not be packed uniformly in the gap; therefore, the heat conduction rate through the sand was not constant.

Because of favorable results obtained when using epoxy in a development calorimeter, it was decided to fill the gap in one of

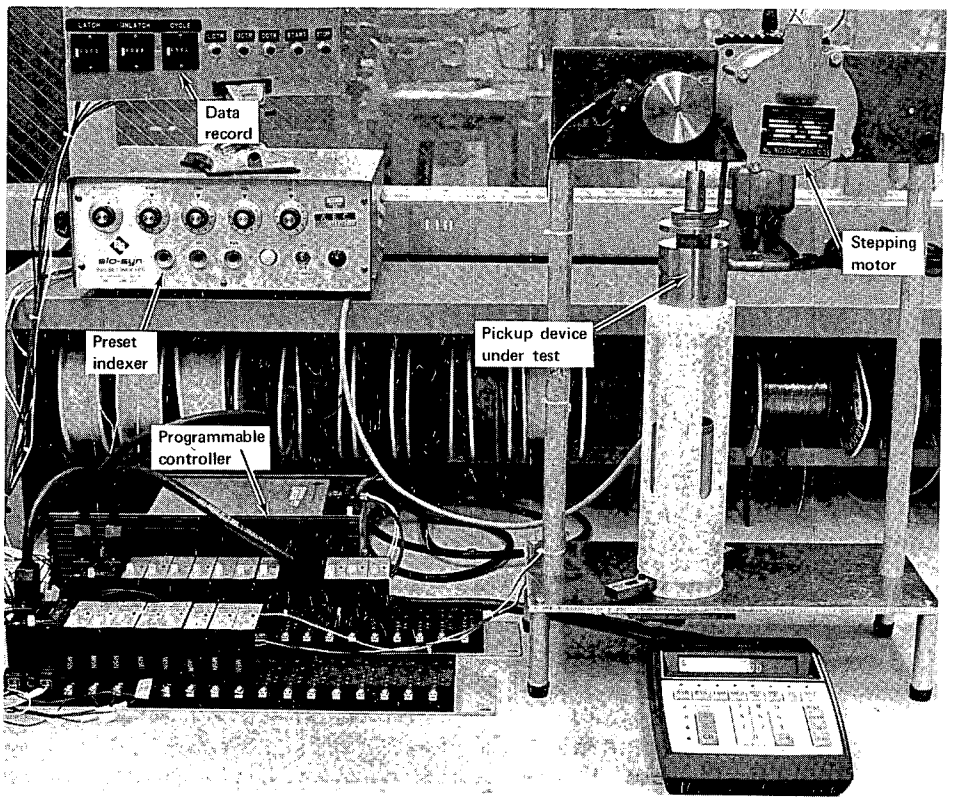

FIGURE 10 - Testing system for cycling pickup devices.

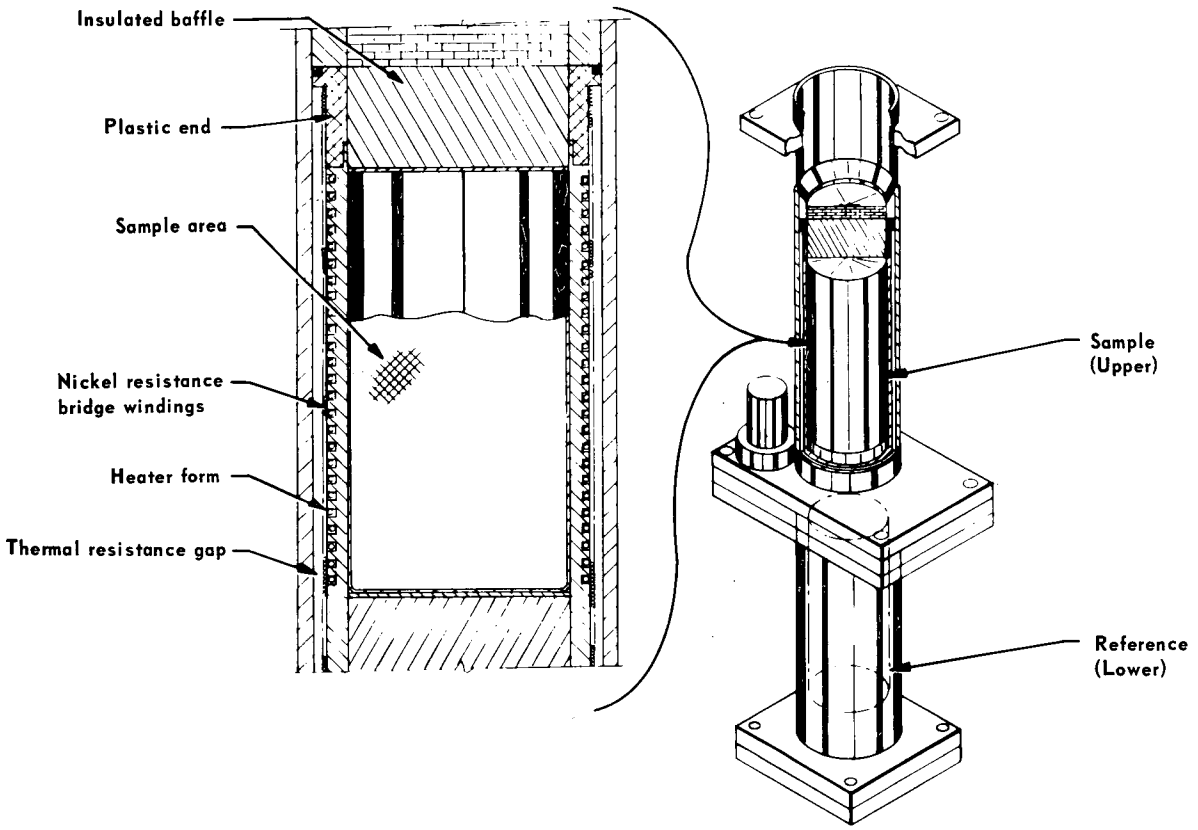

FIGURE 11 - Cross section of Safeguards calorimeter.

the two APAS calorimeters with epoxy (EPON-907). The thermal conductivity of EPON-907 is approximately six times that of air. The gap was filled by building up the outside diameter of the heater form and plastic ends with epoxy and machining this diameter for a slip fit in the brass jacket. Following tests which proved that the epoxy was a satisfactory medium, the gap in the second calorimeter was filled with the same material.

The calorimeters have been tested to determine their sensitivity, thermal resistance, heat distribution error, and reproducibility. The calorimeter sensitivity is equivalent to the sensor output for a unit power input. It is measured by applying a known power through the electric heater and measuring the resulting change in bridge potential. At the same time, a platinum resistance thermometer located in the sample chamber is used to measure the temperature rise across the thermal gradient medium caused by the power from the electric heater. The ratio of the temperature rise to the heater power is a measure of the thermal resistance of the calorimeter.

The heat distribution error was determined by monitoring the bridge potential with a 3-W plutonium-238 heat standard. It was packed in UO_2 and located at various heights in the sample can. The measured results are compared to the true value of the standard to determine the percentage error.

Ten independent determinations of a 3-W heat standard packed in UO_2 were used to measure reproducibility of the calorimeter. The results of all the tests are presented in Table 9. These tests indicate that the epoxy is a suitable thermal gradient medium.

In an additional test, the shape of the sensitivity curve (i.e., calorimeter sensitivity versus input power) was measured over the range of 1 to 15 W. A change in sensitivity of -0.031%/W and -0.028%/W was measured in calorimeters 160 and 161, respectively. This indicates that, although the sensitivity is not constant over the entire wattage range, it is not critically dependent on the power in the calorimeter. The electronics package including controllers for the calorimeter baths, preequilibration baths, and calorimeters as well as the multiplexer for switching the various calorimeter outputs to the computer has been assembled and is undergoing tests. Following satisfactory checkout tests, the electronics package will be interfaced with the calorimeters and the calorimeter system will be tested to determine its accuracy and precision.

Cans

Figure 12 is a drawing of the stainless steel reusable can which has been designed to be compatible with APAS. The can is approximately 16.5 cm high by 6.4 cm in diameter with a 0.08-cm wall thickness. Six of these cans and 50 lids have been fabricated and are being evaluated for compatibility with the X,Y,Z system, calorimeters, and gamma-ray spectrometers. A pickup device has been built to be used with these cans (see page 20). A tool has been designed that could either manually or automatically insert and remove the lids.

The lids are designed to be tamperproof; if a lid is removed, it will be sufficiently damaged or marked that it cannot be reused without being apparent that it had been removed. Initial testing demonstrated that the lids as originally fabricated could be removed without significant damage in about 30 min by carefully prying on the edge with a sharp, thin-bladed tool. However, by machining off approximately two-thirds of the lip of the lid, the lid could not be removed by this technique. Future lids will incorporate this smaller lip.

As a further protection, the cans could also be built with the lid edge being recessed in the top of the can.

Originally, the APAS system was not going to be subjected to extended "hot" testing at Mound Laboratory and was, therefore, assembled in a radioactively "cold" area. More recent guidance indicates the need for some detailed testing at Mound Laboratory with various compositions of reactor fuels. Since the tamperproof reusable can does not provide sufficient containment by itself to be used in a "cold" area, a second can has been fabricated that meets the safety and environmental requirements. This can is basically the

Table 9

TEST RESULTS FOR THE APAS CALORIMETERS

	S/N 160	S/N 161
Sensitivity (5-mA bridge current, 3-W power level):	12,875 μV/W	13,108 μV/W
Thermal Resistance:	0.648°C/W	0.678°C/W
Heat Distribution Errors:		
Top	-0.031%	-0.050%
Middle	+0.030%	+0.001%
Bottom	-0.112%	-0.130%
Precision:	±0.025%	±0.043%

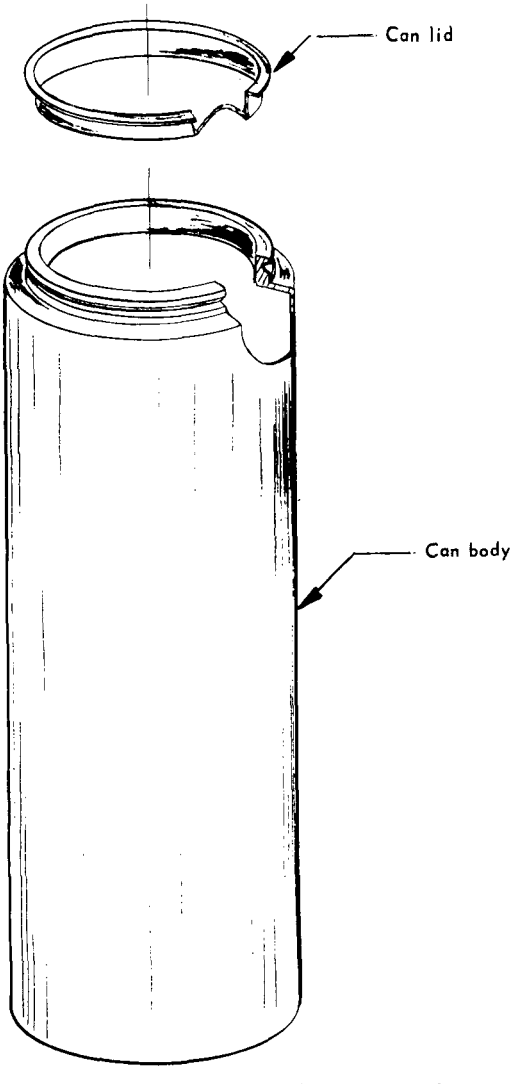

FIGURE 12 - Typical sample can.

same design as the tamperproof can, except that the press-fit lid has been replaced with two screw-on lids. This gives a double O-ring seal for the containment of radioactive material. Twelve of these cans have been made and will be loaded with fuel for use in the extended testing of APAS.

ENGINEERING

Because APAS will be tested in a "cold" area, it is not necessary to house the spontaneous fission assay system (SFAS) in a glovebox. A dummy glovebox has been built to support the X,Y,Z transporter so that the SFAS can be incorporated into the automated sample handling system.

The final drawings of the process calorimeters are complete. Those for the X,Y,Z transporter are approximately 50% complete.

Plates on which the transporter rails will be mounted in a glovebox were designed and built. These plates will provide precision surfaces for aligning and fastening transporter rails while preserving the seal integrity of the boxes.

Applications

PLUTONIUM INVENTORY VERIFICATION PROGRAM

J. F. Lemming, F. X. Haas and J. Y. Jarvis

Two computer programs to facilitate the handling of calorimetric assay data have been written. Both programs are written in FORTRAN II and are run on PDP-8 computers. The first program, ISOTOP, is used to convert gamma-ray peak areas to atom ratios. The nuclear constants used are those of Gunnink and Morrow.[7] The second program, CALDAT, accepts atom ratios and wattage measurements and their uncertainties. It then calculates the total weight of plutonium in grams and its uncertainty. CALDAT uses the recommended specific powers and propagation of the measurement uncertainties from ANSI Standard 15.22 (Calibration Techniques for the Calorimetric Assay of Plutonium-Bearing Solids Applied to Nuclear Materials Control).

Seventy-nine samples and 24 aliquots have been measured in this report period. The categories include: incinerator ash; ash heels; sand, slag and crucibles; sand, slag and crucible heels. Two 1-gal-can calorimeters (149 and 150) were used during the inventory. Standard heat sources were measured before and after the inventory samples. Calorimeter 149 was found to have a bias of -0.13% ± 0.15% at the 1-W power level. Calorimeter 150 has a bias of -0.22% ± 0.15% at the same power level. The calorimeter wattage values were corrected for these biases.

The gamma-ray spectra for the samples and aliquots were acquired on the 70-cc Ge(Li) spectrometer having resolution of 1.8 keV at 1332 keV. The gamma ray spectra were analyzed using the program GAUSS V.

The $^{238}Pu/^{239}Pu$ ratio was measured by radiocounting on 20 aliquots and by spectroscopy on both the aliquots and the 79 cans. Table 10 contains a comparison of the plutonium-238 stream average values determined by each of these methods. Stream averages were determined for each year from 1966 to the present. The agreement of the ratios for each year gives confidence to the assumption of there being a stream average. The radiocounting values with a relative standard deviation of ±6% have been used. The uncertainty is based on a reproducibility of ±3%, over a 3-yr period, for metal exchange samples containing approximately 120 ppm plutonium-238. Since the inventory samples are not metals, the uncertainty was doubled.

The $^{240}Pu/^{239}Pu$ ratio was measured by mass spectroscopy on 20 aliquots. The stream averages determined for each year are shown in Table 10. During the analysis of the aliquots, the electronic integrating circuit malfunctioned and was replaced by an ion pulse counting device. An uncertainty of 1.4% has been used. This value is the relative standard deviation measured on NBS-SRM-948 with the ion pulse counting device.

The $^{241}Pu/^{239}Pu$ ratio was measured by mass spectroscopy on 20 aliquots. Gamma-ray measurements of this ratio were then made on the 24 aliquots and the corresponding samples. The ratio of the gamma-ray to mass-spectroscopic assay for the aliquots is 0.98 ± 0.03. A similar comparison of the gamma-ray measurements on the cans and the corresponding aliquots yields a ratio of 1.01 ± 0.02. The gamma-ray measurements of this ratio on the cans have been used with a relative standard deviation of ±3%.

The $^{241}Am/^{239}Pu$ ratio was measured by gamma-ray spectroscopy on the aliquots and the samples. For those samples containing greater than 150 ppm the comparison of the aliquots to the samples yields a ratio of 1.01 ± 0.07. This is consistent with past results. The ratios determined from the bulk samples have been used with an uncertainty of ±7%. For americium-241 concentrations less than 150 ppm, the aliquots and bulk sample measurements do not agree. These are all in the category of incinerator virgin ash.

Table 10

STREAM AVERAGE ISOTOPIC RATIOS

Year	Number of Aliquots	Number of Samples	$^{238}Pu/^{239}Pu$ Aliquot Radiocounting	$^{238}Pu/^{239}Pu$ Aliquot Gamma	$^{238}Pu/^{239}Pu$ Can Gamma	$^{240}Pu/^{239}Pu$ Mass Spec	$^{242}Pu/^{239}Pu$ Mass Spec
66	1	1	97[a]	83 ± 9[b]	89 ± 8[b]	60280	200
67	1	2	107	109 ± 8	95 ± 6	60600	200
68	1	2	106	106 ± 5	104 ± 5	60890	230
69	1	2	109	106 ± 5	105 ± 7	62370	230
70	1	2	117	103 ± 8	110 ± 16	62810	260
71	3	6	126	126 ± 8	121 ± 14	63279	236
72	0(2)[c]	14		130 ± 3	127 ± 17	63000[d]	260[d]
73	3(4)[c]	10	121	120 ± 7	125 ± 15	63063	257
74	2	12	124	109 ± 5	124 ± 9	63240	270
75	3	10	121	126 ± 1	123 ± 12	63007	267
Current	4(5)[c]	18	117	118 ± 3	113 ± 8	62867	261

[a] Values within ±6%.
[b] Statistical uncertainty if one measurement; otherwise relative standard deviation.
[c] The number of aliquots measured by gamma-ray techniques; mass spectrometer data not available on all samples.
[d] Chosen on the basis of trends of the stream averages.

Based on counting statistics the average uncertainty is ±11% for these bulk samples containing less than 150 ppm. For the audit we have used the ratio determined from the bulk samples with an uncertainty of ±15%.

A series of five gamma-ray spectra was taken of a single sample to check the reproducibility of the gamma-ray isotopic determinations. The relative standard deviation about the mean value for the $^{238}Pu/^{239}Pu$ ratio was ±6%, for the $^{241}Pu/^{239}Pu$ ratio ±1.1%, and for the $^{241}Am/^{239}Pu$ ratio ±3%.

ZPPR FUEL PINS

F. X. Haas and J. F. Lemming

Gamma-ray spectra were obtained in March 1974 on five ZPPR fuel pins when these pins were calibrated by calorimetry.[8] These pins, approximately 3/8 in. (0.95 cm) in diameter by 6 in. (15 cm) long, contained 12 g of plutonium in about 90 g of PuO_2-UO_2. Spectra were obtained on the 70-cc Ge(Li) spectrometer for 20,000-sec counts. The spectra were analyzed using both GAUSS V[6] and GRPANL. For both analyses the plutonium-240 and americium-241 concentrations were determined in the 640-660-keV region. The plutonium-238 concentration was calculated relative to plutonium-241 from the 153-keV/148-keV peaks. The plutonium-241 concentration was calculated from the 208-keV/203-keV peaks.

Table 11 shows a comparison of the isotopic results obtained by gamma-ray analysis to the chemical values supplied with the samples decayed to the gamma-ray analysis date. In both cases, the isotopic ratios agree with the chemical values to within approximately 5%, with the exception of the plutonium-240 value obtained using GRPANL. The last line in this table shows the calculated specific power for these isotopic values. The use of gamma-ray isotopics would yield total plutonium values which are 0.43% and 1.2% (GAUSS V and GRPANL values, respectively) higher than corresponding values using chemical isotopics.

If the gamma-ray isotopic ratios for each pin are used to calculate the specific power for that pin, the mean value for the specific power is 3.234 ± 0.022 mW/g. This means that the contribution from the uncertainty in the gamma-ray isotopic ratios to the overall uncertainty in the calorimetric assay would be approximately 0.7%.

Table 11

AVERAGE ISOTOPIC CONCENTRATIONS AND SPECIFIC POWERS OF FUEL PINS
(ALL VALUES COMPUTED TO THE SAME DATE)

		Average Gamma-Ray Value			
Isotope	Chemical Analysis (ppm)	GAUSS V (ppm)	Difference (%)	GRPANL (ppm)	Difference (%)
^{238}Pu	523	550 ± 36	5.2	556 ± 24	6.3
^{240}Pu	131990	130917 ± 7697	-0.8	118960 ± 7602	-9.9
^{241}Pu	16172	16207 ± 226	0.2	16346 ± 67	1.1
^{241}Am	4473	4245 ± 102	5.1	4372 ± 393	-2.3
Specific Power (mW/g)	3.245	3.231	-0.43	3.206	-1.2

References

1. Nuclear Safeguards Progress Report: July 1974 - June 1975, MLM-2286 (Dec. 19, 1975), pp. 5-15.

2. R. Gunnink, A System for Plutonium Analysis by Gamma-Ray Spectrometry. Part 2: Computer Programs for Data Reduction and Interpretation, UCRL-51577 Part 2, University of California Radiation Laboratory, Livermore, Calif. (Apr. 18, 1974), 98 pp.

3. Mound Laboratory Activities for the Division of Safeguards and Security: January-June 1974, MLM-2186 (Dec. 27, 1974), pp. 6-12.

4. G. Keepin, Nuclear Analysis Research and Development Progress Report, January - April, 1974, LA-5678-PR, Los Alamos Scientific Laboratory, Los Alamos, N.M. (1974), p. 15.

5. R. Gunnink, A Simulation Study of Plutonium Gamma-Ray Groupings for Isotopic Ratio Determinations, UCRL-51605, University of California Radiation Laboratory, Livermore, Calif. (June 10, 1974), 58 pp.

6. R. G. Helmer and M. H. Putnam, GAUSS-V, A Computer Program for the Analysis of Gamma-Ray Spectra from Ge(Li) Spectrometers, ANCR-1043, Aerojet Nuclear Corp., Idaho Falls, Ida. (January 1972), 68 pp.

7. R. Gunnink and R. J. Morrow, Gamma-Ray Energies and Absolute Branching Intensities for $^{238, 239, 240, 241}$Pu and ^{241}Am, UCRL-51087, University of California Radiation Laboratory, Livermore, Calif. (July 22, 1971), 26 pp.

8. MLM-2186, pp. 29-30.

Distribution

EXTERNAL

TID-4500, UC-15

F. J. Arsenault, NRC
N. S. Beyer, ANL
C. D. Bingham, NBL
R. N. Chanda, Rocky Flats
L. L. Cleland, LLL
R. B. Crouch, ERDA/ALO
R. Gunnink, LLL
G. A. Hammond, ERDA/DSS
W. A. Higinbotham, BNL/TSO (3)
R. B. Jones, NRC
S. C. T. McDowell, ERDA/DSS (3)
H. K. Nason, MRC
J. Selleck, NRC
T. E. Shea, NRC
P. Ting, NRC
E. A. Walker, ERDA/DAO (3)
R. B. Walton, LASL
E. V. Weinstock, BNL/TSO
W. H. Zimmer, ARHCO

CONSULTANTS

C. F. Curtiss
University of Wisconsin
C. F. Eck
Miamisburg, Ohio
H. W. Mattson
Monsanto Company
D. F. Griffing
Miami University
R. E. Miers
Ft. Wayne, Indiana
G. W. Powell
Ohio State University
A. Shapiro
University of Cincinnati
H. F. Swift
University of Dayton Research Institute
D. White
University of Pennsylvania

INTERNAL

J. H. Birden
W. T. Cave
C. F. Draut
M. F. Duff
C. L. Fellers (6)
T. K. Ferguson
R. K. Flitcraft
F. X. Haas
C. W. Huntington
J. F. Lemming
J. R. McClain
R. A. Neff (6)
D. O. Page
W. W. Rodenburg
P. W. Seabaugh
D. E. Sellers
W. H. Smith (6)
W. W. Strohm (10)
R. E. Vallee
H. A. Woltermann
Records Center
Library (15)
Publications